

LES, AMR and multiscale modeling for shock driven turbulence

C. Pantano, R. Deiterding, D. Hill and D.I. Pullin, Graduate Aeronautical Laboratories, California Institute of Technology

Introduction

Highly under-resolved yet high-fidelity simulation of compressible turbulent flows driven by strong shocks remains a substantial challenge in modern computational science. The present development adds an advanced physics-based modeling capability for these flows to the Caltech ASC Center's Virtual Test Facility (VTF). Some issues that we address presently include:

- Physical aspects:
 - Need to resolve certain regions of the flow field more finely than others; thin shear layers, shocks and regions of steep density gradients produced by mixing and combustion.
 - Subgrid-scale (SGS) models required for turbulence owing to the limitations imposed by large Reynolds number scaling. This includes subgrid extension of turbulence statistics.
- Numerical aspects:
 - Development of a numerical scheme merging a shock-capturing capability with low-numerical dissipation required for explicit SGS modeling in smooth regions.
 - Robustness and well-posed boundary conditions, both for inflows and outflows, is desirable (characteristic based boundary conditions and stable boundary stencils)
- Computational efficiency aspects:
 - Reduction of computational costs by use of AMR strategies
 - Use of fast linear algebra packages
 - Optimization achieved, for example, by table lookup techniques

We present examples of turbulent flow simulation using LES performed within the block-structured adaptive mesh refinement infrastructure AMROC [3]. A fully compressible formulation of the transport equations and the stretched-vortex subgrid-stress model [5] are integrated with additional SGS models for specific closures.

Subgrid modeling

The stretched-vortex SGS model is utilized [5]. Here it is assumed that subgrid motion is represented by subgrid vortical structures. The required SGS terms are expressed as

$$\tau_{ik} = \bar{\rho}(\widetilde{u_i u_k} - \widetilde{u_i} \widetilde{u_k}) - (\bar{\sigma}_{ik} - \bar{\sigma}_{ik}) = \bar{\rho} k_{sgs} (\delta_{ik} - e_i e_k), \quad (1)$$

for momentum, the subgrid total energy transfer

$$\begin{aligned} \sigma_k^e &= \bar{\rho}(\widetilde{h u_k} - \widetilde{h} \widetilde{u_k}) + \frac{\bar{\rho}}{2}(\widetilde{u_j u_j} u_k - \widetilde{u_j} \widetilde{u_j} \widetilde{u_k}) - (\bar{\sigma}_{k_j} u_j - \bar{\tau}_{k_j} \widetilde{u_j}) + (\bar{q}_k - \bar{q}_k) \\ &= \frac{1}{2} \bar{\rho} \Delta_c k_{sgs}^{1/2} (\delta_{jk} - e_j e_k) \frac{\partial \bar{h}}{\partial x_j}, \end{aligned} \quad (2)$$

and the subgrid scalar transport

$$\sigma_k^l = \bar{\rho}(\widetilde{Y_l u_k} - \widetilde{Y_l} \widetilde{u_k}) + (\bar{J}_k^l - \bar{j}_k^l) = \frac{1}{2} \bar{\rho} \Delta_c k_{sgs}^{1/2} (\delta_{jk} - e_j e_k) \frac{\partial \bar{Y}_l}{\partial x_j}, \quad (3)$$

where e_i are the direction cosines of the subgrid vortex axis and Δ_c is the subgrid cutoff length scale. The subgrid kinetic energy, k_{sgs} , is given by

$$k_{sgs} = \int_{k_c}^{\infty} E(k) dk, \quad (4)$$

where $k_c = \pi/\Delta_c$. The subgrid vortices are assumed to take the form of a Lundgren stretched-spiral vortex with shell-summed subgrid energy spectrum of the form

$$E(k) = \kappa_o \epsilon^{2/3} k^{-5/3} \exp(-2k^2 \nu / (3|\alpha|)). \quad (5)$$

The parameter κ_o is the Kolmogorov prefactor, ϵ is the local cell-averaged dissipation and $\alpha = \widetilde{S}_{ij} e_i^l e_j^l$ is the axial strain along the subgrid vortex axis provided by the locally resolved flow with rate-of-strain tensor

$$\widetilde{S}_{ij} = \frac{1}{2} \left(\frac{\partial \widetilde{u}_i}{\partial x_j} + \frac{\partial \widetilde{u}_j}{\partial x_i} \right).$$

In order to implement the model, the e_i must be specified or otherwise determined, and the composite parameter $\kappa_o \epsilon^{2/3}$ calculated. The e_i are modeled by alignment with extensional eigenvectors of \widetilde{S}_{ij} and with the resolved-scale vorticity. The parameter $\kappa_o \epsilon^{2/3}$ is calculated using resolved-scale, second-order velocity structure functions.

Numerical method

Tuned centered stencil for LES

We use the tuned second order centered scheme (TCD) [4] that consist of an explicit 5-point stencil, tuned to minimize truncation errors in LES simulations. For a uniform one-dimensional discretization at the points $x_j = h_j$, with $j = 1$ to N , the stencil formula for the derivative of $f(x_j)$ is given by

$$\frac{df_j}{dx} = \frac{\alpha(f_{j+2} - f_{j-2}) + \beta(f_{j+1} - f_{j-1})}{h}, \quad (6)$$

where $\beta = 1/2 - 2\alpha$ is required for second order accuracy. The value $\alpha = -0.197$ minimizes LES truncation errors for a flow field with Kolmogorov-type energy spectra [4].

Hybrid centered-upwinded formulation

A key feature of the center's approach to compressible turbulence is the utilization of dynamically adaptive stencil selection. This implies

- TCD stencil used in turbulent regions
- WENO stencil used around shocks
- Smooth transition between schemes guaranteed by choosing the target optimal WENO stencil to be that of the TCD

The choice of stencils (switch) is generally in control of the user. We currently used k-split switch criteria, C^k , based on different techniques depending on the problem,

- Pressure and density curvature
- Entropy condition
- Least-square discontinuity regression
- Non-linear pressure gradient mapping

The switching is done in a direction by direction manner with fine grained control (cell to cell) in terms of fluxes following

$$\mathbf{F}^k = \begin{cases} \mathbf{F}_{WENO}^k, & \text{in } C^k \\ \mathbf{F}_{TCD}^k, & \text{in } \bar{C}^k, \end{cases} \quad (7)$$

where \mathbf{F}^k is the flux vector in direction k .

Stable boundary stencils and boundary conditions

We construct a stable boundary closure [2] of the first order derivative that satisfies the summation by parts property, that in the case of the TCD scheme is given by

$$P \frac{df}{dx} = \frac{1}{h} Q f, \quad \text{with} \quad P = \begin{bmatrix} p_1 & 0 & 0 \\ 0 & p_2 & 0 \\ 0 & 0 & 1 \end{bmatrix}, \quad Q = \begin{bmatrix} -1/2 & q_{12} & \alpha \\ -q_{12} & 0 & \beta \\ -\alpha & -\beta & 0 \end{bmatrix} \quad (8)$$

where f is the vector of discretized values and $q_{12} = 1/2 - \alpha$, $p_1 = 1/2 + \alpha$ and $p_2 = 1 - \alpha$. It can be shown that a suitably defined energy norm is conserved for (8). We also use characteristic based boundary conditions [9] to impose well-posedness at open boundaries. Cancellation of undesired incoming characteristic waves makes open boundaries non-reflective. When the incoming characteristic strength is known, as in inflows, a penalty based technique (SAT) associated with Eq. (8) is used.

Conservative formulation for AMR

Robust LES solvers require stable discretizations, skew-symmetric like. Our approach follows primarily a formulation [1] where convective terms are evaluated as

$$\frac{\partial(\rho u_j \psi)}{\partial x_j} \rightarrow \frac{1}{2} \frac{\partial(\rho u_j \psi)}{\partial x_j} + \frac{1}{2} \rho u_j \frac{\partial \psi}{\partial x_j} + \frac{1}{2} \psi \frac{\partial(\rho u_j)}{\partial x_j}. \quad (9)$$

These modifications apply to the momentum, scalar and energy conservation equations and are typically sufficient to improve stability of the simulations. Conservation in the AMR meshes is achieved by using a flux-based approach with convective and skew-like fluxes given by

$$\begin{aligned} F_{i+1/2} &= \alpha(f_{i+2} + f_{i-1}) + (\alpha + \beta)(f_i + f_{i+1}), \\ F_{i+1/2}^s &= \alpha(a_{i+2} b_i + a_{i-1} b_{i+1} + a_i b_{i+2} + a_{i+1} b_{i-1}) + \beta(a_i b_{i+1} + a_{i+1} b_i), \end{aligned}$$

respectively.

Simulation results

We investigate a Richtmyer-Meshkov instability where a shock interacts with a thin interface starting the acceleration induced mixing of the fluids. The shock reflects off the closed end of a shock tube and 'reshocks' the interface, further driving the now turbulent mixing. This flow exercises both the LES and the shock capturing features of the solver with dynamically adaptive meshes. The results of mixing layer growth rate are compared with the experimental measurements [10] for case Mach 1.5 shock interacting with an Air-SF₆ interface (Fig. 1). The unshocked air has a density of 0.27885 kg/m³ and pressure of 23 kPa. The domain dimensions are $-0.20 \text{ m} \leq x \leq 0.62 \text{ m}$ by $-0.135 \text{ m} \leq y \leq 0.135 \text{ m}$ by $-0.135 \text{ m} \leq z \leq 0.135 \text{ m}$. A perfectly reflecting boundary condition is used at the wall and a characteristic boundary condition is used at the open boundary.

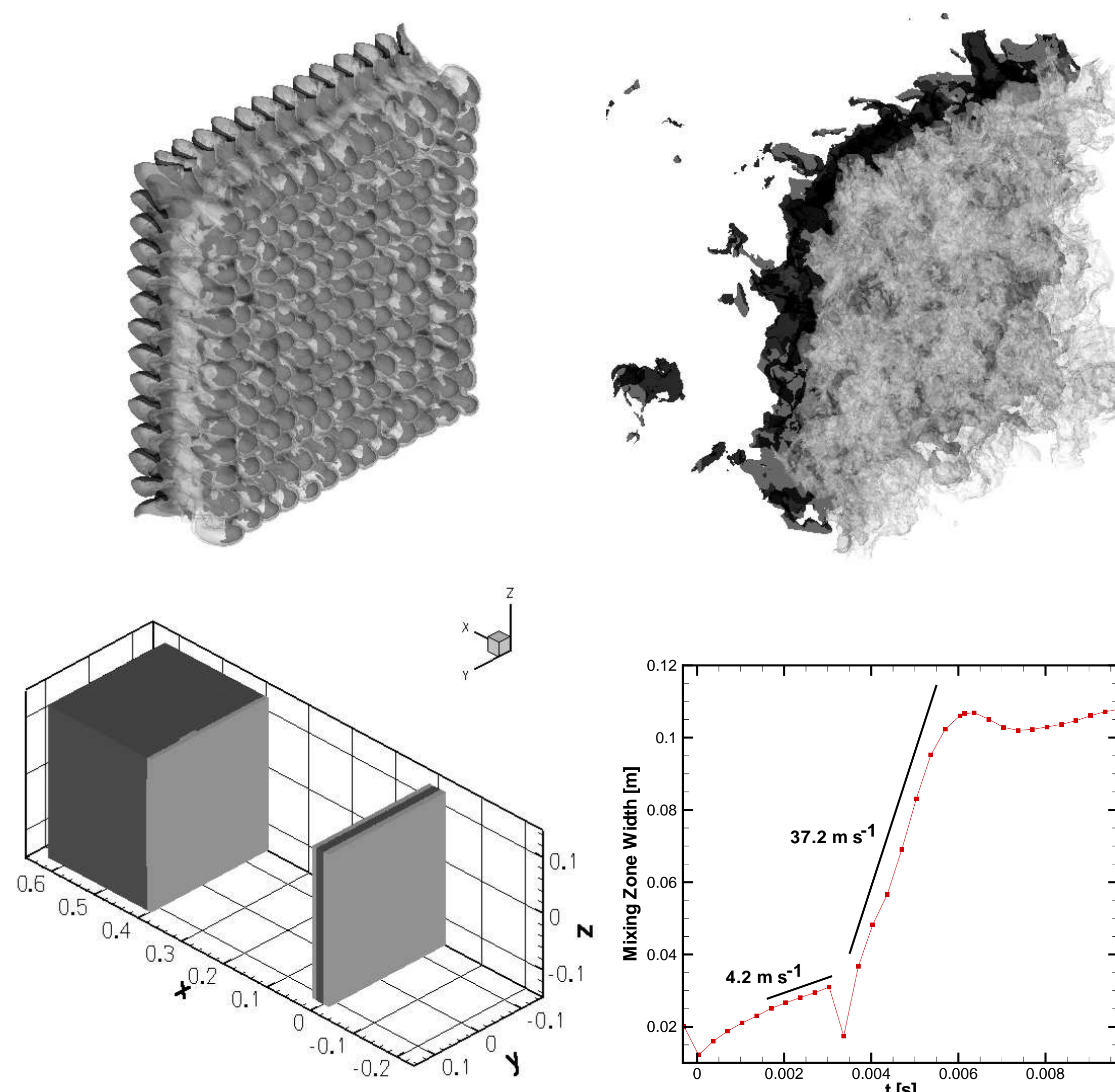


Figure 1: Richtmyer-Meshkov instability simulated with 3 levels of AMR. Isosurfaces of mixture fraction (top) at different times, fine mesh regions (bottom left) and mixing layer thickness (bottom right).

Multiscale modeling

Owing to its structured basis, the stretched-vortex SGS model allows multi-scale modeling of certain statistical quantities via estimation of the contribution to these statistics of scales below the resolved-scale cutoff, including

- True multi-scale modeling: matching of 'inner' and 'outer' scales
- No free parameters employed in matching
- Use stretched model to compute subgrid statistics
- Additional modeling allows prediction of Schmidt number effects on mixing

To illustrate results, Fig.2 (left) shows velocity spectra in the $y-z$ centerplane of the mixing layer some time after reshock. Two-dimensional, circle-averaged (in $k_y - k_z$ space) spectra are shown for both the component of the velocity normal to the $y-z$ plane (w), and in the $y-z$ plane. The subgrid extensions of the resolved-scale spectra can be calculated using the analysis of Pullin and Saffman [7] and are defined by

$$E_{qq}^{2D}(k_r) = \frac{2k_r}{\pi} \int_{k_r}^{|\kappa_r / \cos \alpha_0|} \frac{E(\kappa)}{(\kappa^2 - k_r^2)^{1/2} (k_r^2 - \kappa^2 \cos^2 \alpha_0)^{1/2}} d\kappa, \quad (10)$$

$$E_{33}^{2D}(k_r) = \frac{2k_r}{\pi} \int_{k_r}^{|\kappa_r / \cos \alpha_0|} \frac{(k_r^2 - \kappa^2 \cos^2 \alpha_0)^{1/2} E(\kappa)}{\kappa^2 (\kappa^2 - k_r^2)^{1/2}} d\kappa, \quad (11)$$

where α_0 is the angle made by the vortex axis with the $(y-z)$ -plane within a cell. The subgrid extension of the two spectra match reasonably smoothly onto the resolved-scale spectra and exhibit a similar degree of anisotropy in the out-of-plane ($x \equiv '3'$), compared to the in-plane directions ($2D$ isotropy is expected in the $y-z$ plane).

Fig.2 (right) shows mixture fraction spectra estimated from the resolved scale second-order structure function of the scalar and different levels of mixing, parametrized by the Schmidt number. It is important to point out that, strictly speaking, mixing is not represented in the scales of LES, mixing can only be estimated. An approximate solution to the equations describing the mixing of a passive scalar inside a stretched-spiral vortex [6] is used to obtain the scalar spectrum, which, for the scalar ψ , we express in the form

$$E_\psi(k) = K_\psi \left(k^{-5/3} \exp\left(-\frac{(4\nu + 2D)k^2}{3\bar{a}}\right) + \frac{8}{5\pi} \left(\frac{2\Gamma}{\bar{a}}\right)^{1/3} k^{-1} \exp\left(-\frac{2Dk^2}{3\bar{a}}\right) \right), \quad (12)$$

where \bar{a} is the axial resolved-scale strain rate along the subgrid vortex axis, Γ is the subgrid vortex circulation and K_ψ is a group prefactor whose numerical value depends on physical quantities that describe the internal structure of the vortex and the initial scalar field. Equation (12) is consistent with phenomenological models for scalar mixing in turbulence; see [8].

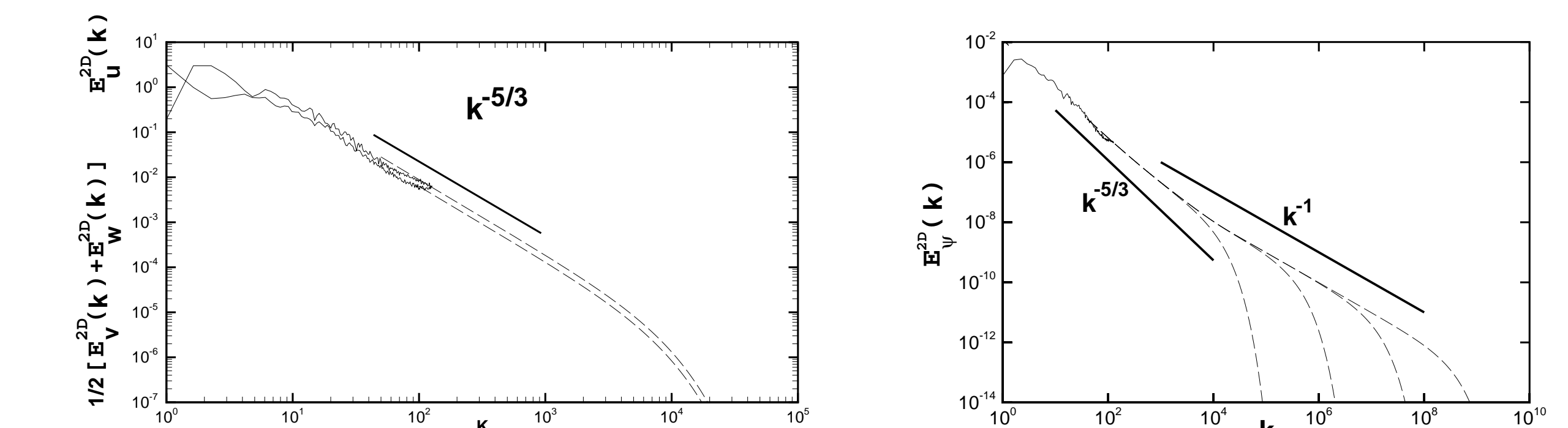


Figure 2: 2D planar isotropic (v, w across the tube) and anisotropic (u) spectra across the center of the turbulent mixing zone (TMZ) (left). Radial scalar spectra with subgrid continuation (broken lines) assuming, from left to right, $Sc = 1, 10^3, 10^6, \text{ and } 10^9$ (right).

References

- G.A. Blaisdell. *Numerical simulation of compressible homogeneous turbulence*. PhD thesis, Stanford University, 1991.
- M.H. Carpenter, D. Gottlieb, and S. Abarbanel. Time-stable boundary conditions for finite difference schemes solving hyperbolic systems: Methodology and application to high-order compact schemes. *J. Comput. Phys.*, 111:220, 1994.
- R. Deiterding. *Parallel adaptive simulation of multi-dimensional detonation structures*. PhD thesis, Techn. Univ. Cottbus, Sep. 2003.
- D.J. Hill and D.I. Pullin. Hybrid tuned center-difference-weno method for large eddy simulations in the presence of strong shocks. *J. Comput. Phys.*, 194(2):435–450, 2004.
- A. Misra and D.I. Pullin. A vortex-based subgrid stress model for large-eddy simulation. *Phys. Fluids*, 9(8):2443–2454, 1997.
- D. I. Pullin and T. S. Lundgren. Axial motion and scalar transport in stretched spiral vortices. *Phys. Fluids*, 13:2553–2563, 2001.
- E.I. Pullin and P. G. Saffman. Reynolds stresses and one-dimensional spectra for a vortex model of homogeneous anisotropic turbulence. *Phys. Fluids*, 6:1787–96, 1994.
- H. Tennekes and J. L. Lumley. *A first Course in Turbulence*. MIT Press, Cambridge, MA, 1974.
- Kevin W. Thompson. Time Dependent Boundary Conditions for Hyperbolic Systems. *J. Comput. Phys.*, 68:1–24, 1987.
- M. Vetter and B. Sturtevant. Experiments on the richtmyer-meshkov instability on a air/sf6 interface. *Shock Waves*, 4(5):247–252, 1995.

